



**5-3-17 AN EXPERIMENTAL STUDY ON THE EXTERNAL LOAD
ACTING ON BASEMENT DURING EARTHQUAKES**

Yutaka SEYA¹, Kyouichi OMATSUZAWA¹, Takafumi ITOH¹
Munekazu MIYAKI², Yoshio SUZUKI³ and Hiroshi TSUNEKAWA³

¹ Tokyo Electric Power Service Co., Ltd. Minato-ku, Tokyo, Japan

² Takenaka Corporation Chuou-ku, Tokyo, Japan

³ Takenaka Technical Research Laboratory Koto-ku, Tokyo, Japan

SUMMARY

The external load due to earthquakes as determined by the current code on aseismic design of buildings in Japan is apt to be overestimated. In this study, we have investigated the dynamic behavior of soil-structure system using shaking table tests on models to obtain a better understanding of the external load. All the models were tested in the elastic region. Both frequency response tests and random tests using simulated waves were carried out on the shaking table. Through our study, we collected as much data as possible to get a better grasp of the external load on the basements. In addition, the experimental results were compared with the results from a 3-dimensional finite element analysis.

INTRODUCTION

As per the building code in Japan, the external load due to earthquakes on the superstructure must be calculated using "coefficient of story-shearing force". The code also stipulates that the load on the substructure should be calculated using "horizontal intensity". If buildings are designed according to this code, the story-shearing force increases from the ground surface to the bottom of the building below the ground surface. If we are able to estimate the story-shearing force on the basement more accurately, we can then design buildings more rationally. We have made attempts to estimate the story-shearing force on basements by experiment and well established numerical analysis tools.

EXPERIMENT

Experimental models Fig.-1 shows the experimental model. The ground model is made of an elastic material, silicon rubber. The ground model is enclosed within a shear ring made of a hard plastic plate covered with teflon. The ring allows the ground to move by shear force only.

The basement model is buried in the ground model. It has at most 4 stories. A set

of plate springs is used to connect the stories to one another. At each story acceleration, story-shearing force, relative displacement and earth pressure can be independently measured. The stiffness of the basement can be changed by the plate springs.

The superstructure model is made of a pair of plate springs with loads attached to them. The natural frequency of the superstructure can be changed by adding to or removing some of the loads from the plates. The superstructure model is connected to the basement model at ground level.

Experimental cases Fig.-2 shows the various cases that were tested experimentally. The parameters are (1) the stiffness ratio between that of the surrounding ground, G_s , and of the basement, G_{BL} and (2) the ratio of natural period of the surrounding ground, T_s , and that of the superstructure, T_B . The stiffness ratio, G_s/G_{BL} , was used for soil classification and its value was taken as 2.0, 1.0 and 0.3. The building classification was done by means of the ratio of natural period, T_s/T_B , which was taken to be 2.0, 1.0 and 0.7.

Method of experiment Two different types of tests, the frequency response test and a simulated earthquake shaking test were conducted. The frequency response test is done by sweeping across the frequency range from 5 Hz to 35 Hz with the input acceleration set at 50 gals. The simulated earthquake wave was generated from a response spectrum which was kept constant in the target frequency range. The input motion was adapted to meet the characteristics of the shaking table but care was taken to ensure that the spectral values are not below 200 gals in the target frequency range.

RESULTS FROM FREQUENCY RESPONSE TESTS

Basement only Fig.-3 shows the test results at 13.5Hz which corresponds to the natural frequency of the soil. The maximum acceleration of the basement is the same for all the building types. The earth pressure and story-shearing force increase as the stiffness ratio, G_s/G_{BL} , decreases. The earth pressure near the ground level always works to the same direction of the displacement of the building.

Superstructure and basement Fig.-4 shows the test results for R-C-1 at 25Hz which corresponds to the natural frequency of the superstructure. The earth pressure at the 1st story of the basement supports the building. The story-shearing forces on the basement are smaller than on the superstructure. The story-shearing forces on the basement decrease with depth below the ground surface. The higher the building, the larger is the earth pressure near the ground. Similar results are obtained at 13.5 Hz, the natural frequency of the soil.

Fig.-5 shows the results for R-C-3 at 13.5Hz. The measurements on the building are out of phase by 180° with respect to those on the surrounding soil. The distribution of the story-shearing forces on the basement are the same as for the "basement only" case except for the story-shearing force at the 1st story, and even this value is almost the same.

RESULTS FROM RANDOM SHAKING TESTS

Maximum story – shearing force Fig.-6 shows the distribution of the maximum story-shearing forces for the cases when the stiffness ratio is the same.

The maximum story-shearing forces on the superstructure are seen to be independent of the stiffness ratio while those on the basement depend on it. The weaker the soil, the larger are the maximum story-shearing forces. The maximum forces are nearly the same irrespective of the building classification. This suggests that the story-shearing forces and the earth pressure during earthquakes are determined by the soil classification, and not by the building classification.

Relation between story shearing force on superstructure and 1st story of basement

Fig.-7 shows the scattergram of the story-shearing force on the super structure versus that on the 1st story of the basement at each sampling time for R-C-3. The slope of the regressed line is 0.4. It indicates that 60% of the story-shearing force on the superstructure and a similar amount of the inertial force on the 1st story of the basement is the result of the earth pressure of the soil. Fig.-8 shows similar regressed lines for the various cases. The story-shearing force on the 1st story of the basement is smaller than that on the superstructure for all cases except case R-C-1. This behavior is more pronounced as G_s/GBL becomes larger or as T_s/TB becomes smaller.

Ratio of side friction Fig.-9 shows the scattergram of the total earth pressure versus the side friction on the 1st story of the basement at each sampling time. This indicates that the 1/3 of the total earth pressure is the result of side friction. A similar behavior is observed in all the other cases.

FEM ANALYSIS

We carried out a FEM analysis of the experimental models using two programs, FLUSH, 2-D, and SIGNAS, 3-D. Fig.-10 shows the input acceleration wave, which is the same as the acceleration of the shaking table measured during the experiment. As the input is the same we can compare test results with the results from FEM analysis.

FLUSH Fig.-11 shows the FEM model. The soil is modeled by plane strain elements. It has 5 layers. The building is modeled by beam elements. Its mass is lumped at each node of each story. The parameters used in the analysis were measured during the experiment or were calculated from the measured values. The shear ring is modeled as a concentrated mass at the end of the soil model. We used viscous boundary in the out-of-plane direction for modeling the 3-dimensional nature of the problem.

R-A-0, R-B-0 and R-C-0 (no basement cases) and R-C-1, R-C-2 and R-C-3 (weak ground cases) were analyzed. Fig.-12 shows the distribution of the maximum acceleration at each story of the building on weak ground cases. The numerical results match well with the test results for accelerations measured under the ground for each case. The same thing can be said about the superstructure for case R-C-2. But for cases R-C-1 and R-C-3 the numerical results are smaller than the test results for accelerations measured

on the superstructure.

Fig.-13 and Fig.-14 show the frequency response function of acceleration of the 1st story of the basement with respect to the input motion. The bold line indicates the numerical results. The peak frequency and the magnification at the peak frequency is higher for the numerical analysis than for the test results. This effect is probably an artifact of the 2-dimensional nature of the model using FLUSH.

SIGNAS Fig.-15 shows the FEM mesh of the model which is reduced geometrically to 1/4 considering symmetric condition. The surrounding soil has 5 layers (as in the FLUSH model) and it is modeled by solid elements. Friction motion between the shear rings are simulated using solid elements. Beam elements are used to model the building whose mass is lumped at each story level (as in the FLUSH model). The beam elements which model the slabs were taken to be rigid in comparison to the other beam elements. The rest of the parameters used in the analysis are the same as the ones used in FLUSH.

Fig.-16 shows the frequency response functions of various quantities with respect to the input acceleration for analysis case R-C-1. The bold line indicates the numerical results while the lighter line represents the experimental results. The peak frequency and response magnification calculated numerically match the test results (compare this with the results of FLUSH). The peak value at the natural frequency of the building from SIGNAS is smaller than one of test results. But we can identify the peak. On the other hand, the peak cannot be found from the result of FLUSH. Another peak found at 18Hz in the numerical results is probably due to the reflection at the boundary between the soil model and the shear ring.

Fig.-17 shows the frequency response function of the side friction with respect to the input acceleration. Its characteristics are the same as those for the earth pressure with the difference that now the response values are roughly half those of the earth pressure.

CONCLUSIONS

Experiment The story shearing force on the superstructure is independent of the ratio of the stiffness of the surrounding soil and the basement. The shear force on the basement depends on the above stiffness ratio and it has more or less the same value irrespective of whether a superstructure is present or absent except for the story near the ground surface. The surrounding soil supports the building during the earthquakes except for the case of a low building on hard ground.

Simulation analysis The maximum values of various response quantities calculated from the numerical model using FLUSH agreed well with the test results. However, the match wasn't so good in the frequency domain. Calculation using SIGNAS gave good results in the time and frequency domains. In addition, the results of SIGNAS can be used in estimating the side friction.

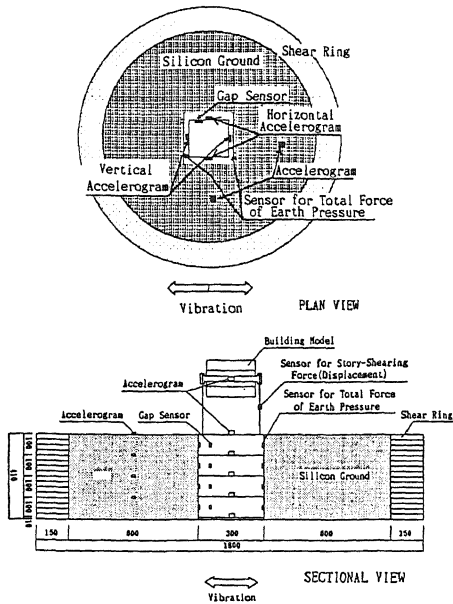


Fig-1 Experimental Model(DIRECT)

Ground Type Case Gs/G _{BL}	Direct		
	A	B	C
2.0 Hard	R-A-0	R-B-0	R-C-0
1.0 Medium	R-A-1	R-B-1	R-C-1
	R-A-2	R-B-2	R-C-2
0.7 Soft	R-A-3	R-B-3	R-C-3

Basement Only: 0 (Low), 1 (Medium), 2 (High)
 Superstructure and Basement: 1 (Low), 2 (Medium), 3 (High)

G_s: stiffness of soil
 G_{BL}: stiffness of building
 T_s: natural period of soil
 T_B: natural period of building

Fig-2 Experimental Cases (Direct Foundation)

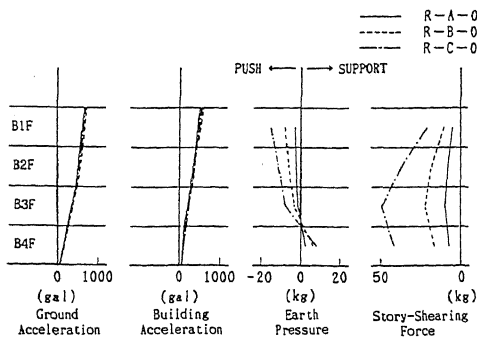


Fig-3 Frequency Response Test Results for Basement Only at 13.5Hz

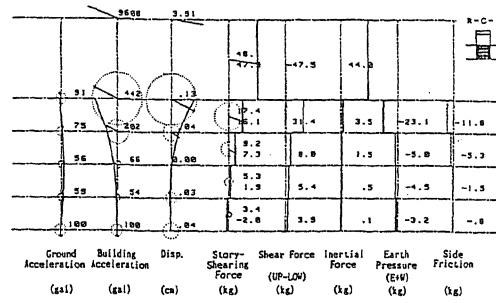


Fig-4 Frequency Response Test Results for R-C-1 at 25Hz

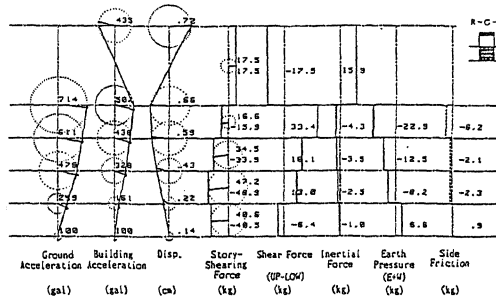


Fig-5 Frequency Response Test Results for R-C-3 at 13.5Hz

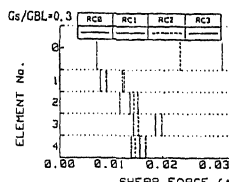
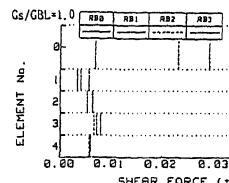
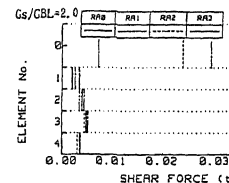


Fig-6 Distribution of the Max. Story-Shearing Forces

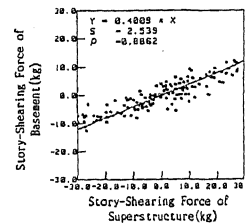


Fig-7 Relationship between Story-Shearing Force on Superstructure and Basement for R-C-3

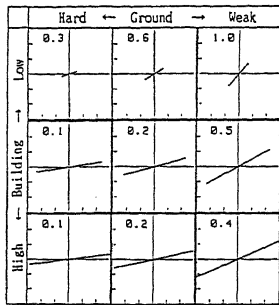


Fig.-8 Relationship between Story-Shearing Force on Superstructure and Basement

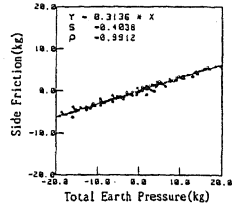


Fig.-9 Relationship between the Total Earth Pressure and Side Friction

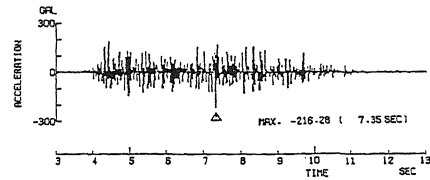


Fig.-10 Input Acceleration

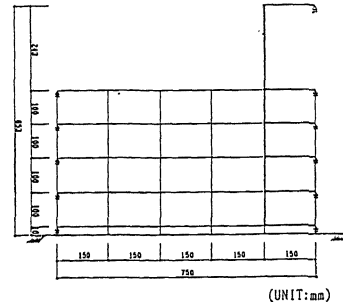


Fig.-11 FEM model (FLUSH)

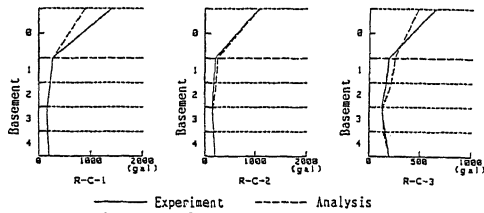


Fig.-12 Distribution of the Max. Acceleration of Building

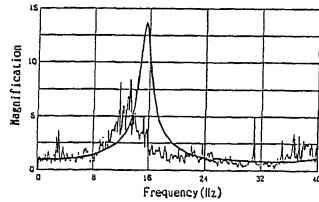


Fig.-13 Acceleration Transfer Function of G.L.

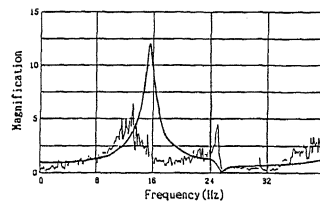


Fig.-14 Acceleration Transfer Function of B1F

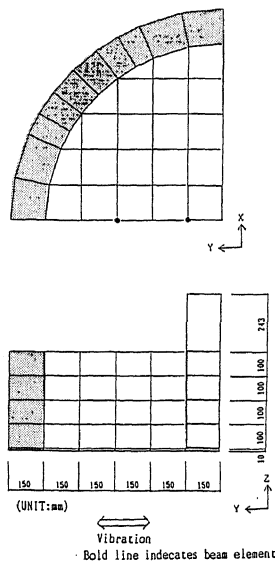


Fig.-15 FEM model (SIGNAS)

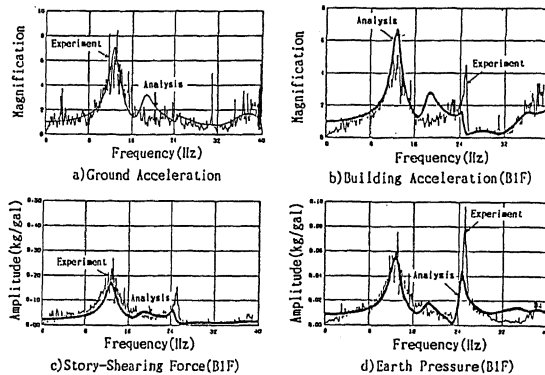


Fig.-16 Frequency Response Function with respect to Input Acceleration

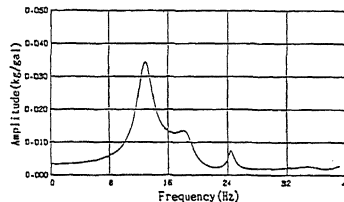


Fig.-17 Frequency Response Function of Side Friction